Pergamon

Scripta Materialia, Vol. 34, No. 4, pp. 579-584, 1996
Elsevier Science Ltd

1359-6462/96 $12.00 + .00

0956-716X(95)00555-2

# HYPERCOOLING OF AN ORGANIC ALLOY MELT

A. Ludwig
Giesserei-Institut der RWTH Aachen
52056 Aachen, Germany

(Received June 27, 1995)
(Revised August 29, 1995)

## Introduction

In recent years, the undercooling of metallic melts under the equilibrium solidification temperature has continued to gain in significance (1,2). Beside the fascination of having a material still in the liquid state, although it should, under normal conditions, already be solid, there are numerous scientific and technical reasons for the increasing interest at this metastable state of liquids. On one hand, fundamental aspects of nucleation (3), crystal growth (4) and thermophysical properties of metastable systems (5) can be investigated. On the other hand, due to phenomena involved in solidification from undercooled melts, like the appearance of metastable phases (6), grain refinement (7,8), reduced microsegregation (9) etc., there exists an interesting potential for the production of new materials (10,11).

Nowadays, there are several means of undercooling a melt. Depending on the thermophysical properties of the material involved, the use of either levitation, drop tube, dispersion, flux or embedding techniques are to preferred. A description of the different techniques can be found in the recent review article from D.M. Herlach et al. (2).

Much of today's knowledge about the solidification of metals has been received from the study of transparent, organic, metal like solidifying liquids (12,13). These materials crystallise with a planar, cellular, dendritic or eutectic morphology, depending on the concentration and the process conditions involved. Since the classical experiments by M.E. Glicksman et al. in 1976 on succinonitrile (SCN) (14), it is well known, that the organic melts can also be undercooled. The highest undercooling which has been achieved with SCN is about 10 K (14,15). By the direct observation of dendrite tips growing into an undercooled melt, Glicksman and co-workers measured the tip radius and the solidification velocity simultaneously (14). They showed, that the hypothesis of maximal growth rate is wrong, initiating with this result a flood of theoretical work (16-20) which has determined today's understanding of dendritic growth, even for metals.

Due to the release of the latent heat of fusion, the solidification of an undercooled melt is accompanied by a rapid increase of temperature, the so called recalescence. Usually the temperature rises rapidly up to the melting point, followed by a slow decrease, during which the residual melt solidifies under equilibrium conditions. However, if the undercooling is higher than the so called Hypercooling limit, the whole liquid transforms into a solid state under non-equilibrium conditions favouring solute trapping and eventually partitionless solidification. This limit was exceeded first in 1990 in pure Ni by Atwater et al. [21]. Vinet at al. undercooled Re by about 975 K [22], which is fare beyond the hypercooling limit of Re, which is

about 600K#. It is believed by the author, that there are at least two groups of researchers, who are in process of publishing experimental evidence for the existence of metallic alloy melts in a hypercooled state (23,24). In this paper, experimental results are presented which show, for the first time, that the Hypercooling limit can be exceeded for organic, metal like solidifying liquids as well. A measurement of the thermal expansion coefficient for the undercooled liquid up to and even beyond the Hypercooling limit is reported.

## Experimental Procedure

The undercooling experiments were performed using a diluted Succinonitrile (SCN)-Argon alloy, which had a measured solidus-liquidus temperature interval of $\Delta T_0 = 480 \pm 50$ mK, which corresponds to $C_0 =$ 0.026 wt.%. Long, fine capillary tubes, made out of borosilicate, which had an inner square cross section of 200 x 200 μm2 and a wall thickness of 100 μm, were filled with the organic material. Further details concerning the purification and filling procedure are given elsewhere (26).

The filled tubes often revealed gas bubbles, which separated the melt into segments of different lengths. Such a segment was surrounded with an isothermal environment, which was realised by placing a 80 mm long section of the tube in a water-jacket of about 80 x 80 x 28 $mm^3$. The height of the water jacket was restricted to 28 mm, because it had to fit under an optical microscope to observe the solidification. The temperature in the centre of the jacket was measured with a quartz thermometer. The detector of this thermometer was cylindrical in shape, about 15 mm in length and 10 mm in diameter. The capillary tube was aligned parallel to the quartz thermometer with a spacing between them of 15 mm. The thermostat used to heat the water flowing though the jacket, as well as the thermometer, had a relative accuracy of 5 mK. The temperature within the jacket was found to vary by about 15 mK. Thus the relative accuracy of the whole system was estimated to be about 20 mK.

To ensure that no pressure due to expansion during melting occurred within the tube, the SCN was molten at the end of the capillary tube (here a larger cavity was present) and then the molten zone was moved towards the segment of interest. The results presented in this publication were obtained from a segment of 30 mm in length. The undercooling and subsequent solidification was observed with an optical microscope, to which a video recorder was attached.

Two different types of undercooling experiments were performed:

(a) To estimate the maximal undercoolability of the SCN-Ar alloy melt, the temperature of the isothermal environment was initially set to $T_0 = 59$°C ($\cong T_L + 0.9$ K), then quickly decreased with a cooling rate of $\dot{T} = 1$ K/s and then hold at a constant predetermined temperature $T_u$. The sudden temperature change from $T_0$ to $T_u$ was realised by using two thermostats and changing the in- and output at the water jacket from one thermostat to the other. After less than 30 seconds the quartz thermometer in the centre of the jacket showed the new temperature. Then all conditions were maintained constant until a nucleation event occurred. Due to the high growth rates produced at high undercoolings, the advance of the solid-liquid interface could not be observed. However the solidification event could clearly be detected, by means of the sudden contraction of the material, which was visible either by the movement of the boundaries of the undercooled segment or by the sudden appearance of cavities. The time interval between the change from $T_0$ to the nucleation event was measured as nucleation time.

(b) In order to estimate the thermal expansion coefficient of the undercooled SCN-Ar melt, γ, the length of the isolated segment was measured, during continuous cooling. The temperature of the water

# Here $C_0$ is calculated considering the phase diagram of Chopra (25) and assuming a constant distribution coefficient of $k$=0.2 and a constant liquidus slope of $m$=-4.7 wt%/K.

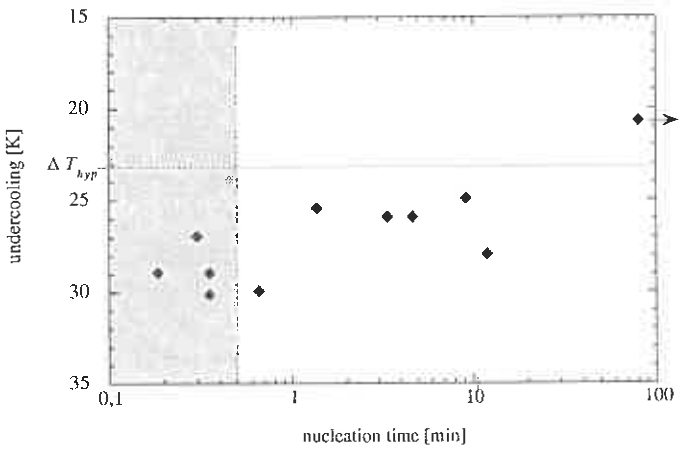


Figure 1. Undercooling vs. nucleation time for selected undercooling experiments. The Hypercooling limit is clearly exceeded. The temperature drop from $T_0 = 59$°C to a prescribed undercooling temperature $T_u$ took about 30 sec. Thus nucleation times of less than 30 sec cannot be taken as reliable (grey area). The undercooling experiment of $\Delta T = 20.7$ K was stopped after 80 minutes, without a solidification event.

within the jacket and thus the temperature of the melt was decreased, simply by switching off the thermostat and the water circulation. The position of the left and right meniscus of the undercooled melt segment was measured as a function of temperature. The difference of the two positions, interpolated to the same temperature, was taken as the length of the segment. Due to the constant segment cross section, the relative length change of the liquid was equivalent to its relative volume change.

## Results and Discussion

Figure 1 shows the maximal achieved undercooling as a function of nucleation time for several undercooling experiments. The experiments, in which the nucleation took place within a time interval of less then 30 seconds should not be considered reliable, because they had not reached a stable temperature. Under the assumption of constant $C_P$, the Hypercooling limit is given by:

$$\Delta T_{hyp} = \frac{L}{C_p} \tag{1}$$

where $L$ is the heat of fusion and $C_P$ the specific heat at constant pressure. Assuming that the Hypercooling temperature is far above the glass transition temperature of SCN, $L$ and $C_P$ can be taken at the melting point. Thus for SCN, where $L = 3.705 \times 10^3$ J/mole (27) and $C_P = 160.1$ J/mole/K (27), Hypercooling is reached when the undercooling is larger than $\Delta T_{hyp} = 23.14$ K. This limit is also shown in Figure 1. During six experiments the Hypercooling limit of SCN was clearly exceeded. The contribution of capillarity effects within the edges of the square cross section tube can be approximated with $\Delta T_r = 2\Gamma/r \cong 120$ mK, with radius of the edge $r = 1$ µm and Gibbs-Thomson-coefficient $\Gamma = 6.22 \times 10^{-8}$ Km (26). Thus the undercooling must be regarded as fully thermal.

The cavities, which occurred after solidification of the highly undercooled SCN-Ar melt were classified in three different ways:

I) detachment of the alloy from the tube walls

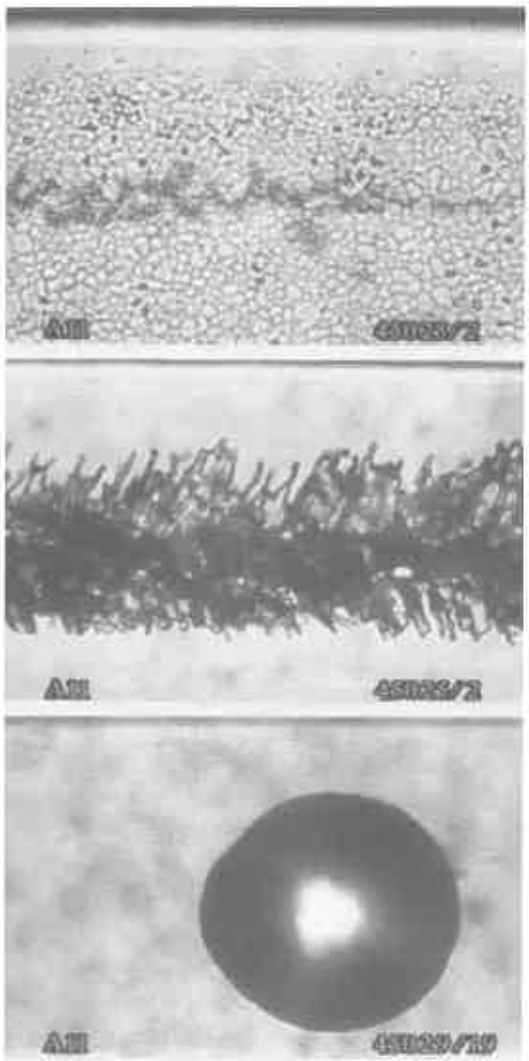

Figure 2. Examples of the three types of cavities which occurred after solidification of the highly undercooled SCN-Ar melt: the detachment of the solid from the tube walls (a), an axial cavity in the centre of the tube (b) and a spherical cavity (c). The cavity-solid interface morphology in (a) and (b) has already coarsed.

II) axial cavities with very irregular boundaries appearing in the centre of the tube
III) spherical cavities randomly distributed within the solid.

Examples of these three classes of cavities are shown in figure 2 a-c. The axial cavities, as well as the detachment of the solid from the tube walls, revealed a fine cavity-solid interface morphology, which, immediately after forming, started to coarsen. Because the photographs, shown in figure 2 a-b, were taken with a delay of a few seconds after solidification, the interface morphology had already became coarser.

The most frequently observed cavity was the detachment of the solid from the tube walls. Figure 2 shows a view from above onto a detached solid region. The unsharp underlying structure in the middle of the picture shows an axial cavity (type III) in the centre of the tube. Whether the grain like structure on

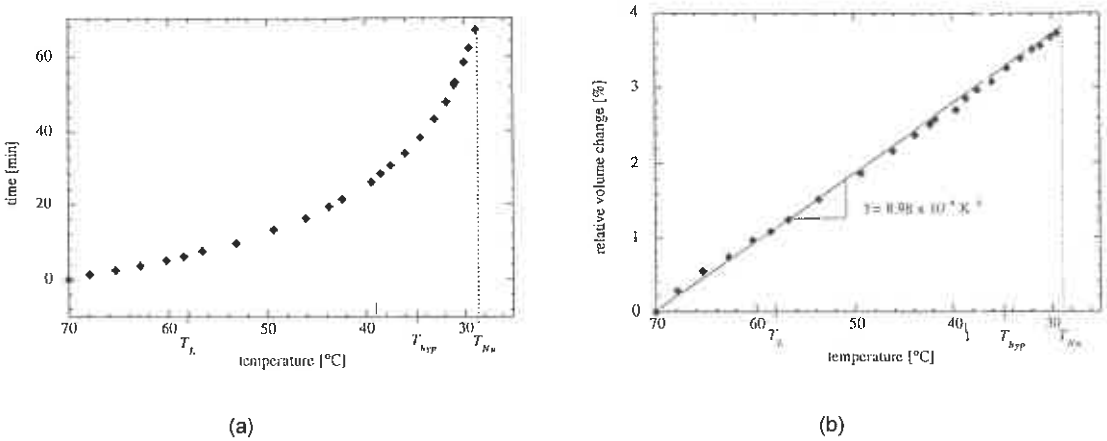


Figure 3.(a) Inverse cooling curve of the centre part of the water jacket. Nucleation occurred at $T_{Nu} = 28.8°C$, which represents an undercooling of $\Delta T_{Nu} = 29.2$ K (6.1 K beyond the Hypercooling limit). (b) Relative volume change of an isolated segment of liquid SCN-Ar alloy vs. temperature. From the slope of the straight line, the thermal expansion coefficient of the undercooled melt is estimated to be $\gamma = 8.98 \times 10^{-4}$ K$^{-1}$.

the surface of the detached solid (fig. 2 a) originated directly from solidification or subsequently from recrystallisation (due to the large defect density of rapidly solidified materials) or from grain refinement (due to dendrite fragmentation) could not be determined from these experiments.

The spherical cavities look like classical gas porosities (fig. 2c). Their appearance might be a hint on solute trapping during solidification - after being trapped from the solid the Argon, now within a supersaturated solid, started to form randomly distributed pores. However, an evolution of the spherical cavities was never observed. Whenever they did occur, they had already attained their final sizes and shapes. Sometimes the spherical cavities occurred together with the detachment from the walls (type I), but they were never found together with the axial cavities (type II).

The axial cavities with their irregular morphology were only observed in the experiments, in which the temperature was slowly reduced ($\gamma$ estimation). Nevertheless they were present even when the undercooling had exceeded the Hypercooling limit. Up to now no systematic explanation for the appearance of the different cavity types is available.

Figure 3 shows the inverse cooling curve (a) and the relative volume change as a function of temperature (b). Due to the slow cooling rate, the temperature within the undercooled segment located close to the quartz thermometer, and the temperature of this detector was assumed to be equivalent. The experiment was started at 70°C, ($\triangleq T_L$ + 12.0 K). The nucleation occurred at $T_{Nu} = 28.8°C$. Thus an undercooling of 29.2 K was achieved. The experiment took more than one hour with an average cooling rate of $\dot{T} = 0.6$ K/min. Within the limits of experimental accuracy, the relative volume change turned out to be a linear function of temperature with a constant slope over the whole temperature range, from above liquidus down to an undercooling beyond the Hypercooling limit. Particularly no deviation from linearity was found at $T_L$ and at $T_{hyp}$. Thus the thermal expansion coefficient, $\gamma$, of the liquid SCN-Ar alloy does not change from above the melting point to the undercooled state. From a linear regression of the experimental points, $\gamma$ was estimated to be $\gamma = 8.98 \times 10^{-4}$ K$^{-1}$. A constant thermal expansion coefficient within the superheated and undercooled liquid was also found for nickel by using the levitation technique (29).

## Acknowledgement

The author is very grateful to W. Kurz for many stimulating discussions, to J. Stramke for his professional assistance, to P.R. Sahm for his personal support and to D.M. Herlach and I. Egry for carefully reading the manuscript. This work was done during a research stay at the EPFL Lausanne, with grant aid from by the Deutsche Forschungsgemeinschaft under Lu 495/1, for which the author kindly acknowledge.

## References

1. *Science and Technology of the Undercooled Melt,* Hrsg.: P.R. Sahm, H. Jones, C.M. Adam, Martinus Nijhoff Publishers (1986)
2. D.M. Herlach, R.F Cochrane, I. Egry, H.J. Fecht, A.L. Greer, Int. Met. Rev. **38** 273 (1994)
3. J.H. Perepezko, Mater. Sci. Eng. **65** 125 (1984)
4. R. Willnecker, D.M. Herlach, B. Feuerbacher, Appl. Phys. Lett. **56** 324 (1990)
5. S. Sauerland, K. Eckler, I. Egry, J. Mater. Sci. Lett. **11** 330 (1992)
6. E. Schleip, D.M. Herlach, B. Feuerbacher, Europhys. Lett. **11** 751 (1990)
7. R. Willnecker, D.M. Herlach, B. Feuerbacher, Phys. Rev. Lett. **62** 2707 (1989)
8. M. Schwarz, A. Karma, K. Eckler, D.M. Herlach, Phys. Rev. Lett. **73** 1380 (1994)
9. K. Eckler, R.F. Cochrane, D.M. Herlach, B. Feuerbacher, Mater. Sci. Eng. **A133** 702 (1991)
10. J. Stanescu, P.R. Sahm, J. Schädlich-Stubenrauch, A. Ludwig, in Proc.: *40th Annual Technical Meeting: Investment Casting Institute*, 29:1 (1992)
11. A. Ludwig, I. Wagner, J. Laakmann, P.R. Sahm, Mat. Sci. Eng. **A 178** 299 (1994)
12. B. Billia, R. Trivedi in *Handbook of Crystal Growth*, Vol. 1B, 901, ed D.T.J. Hurle (Elsevier Science Publishers, Holland, 1993)
13. M.E. Glicksman, S.P. Marsh in *Handbook of Crystal Growth*, Vol. 1B, 1075, ed D.T.J. Hurle (Elsevier Science Publishers, Holland, 1993)
14. M.E. Glicksman, R.J. Schäfer, J.D. Ayers, Met. Trans. **A7** 1747 (1976)
15. M.E. Glicksman, private communication, april 1995
16. J.S. Langer, H. Müller-Krumbhaar, J. Crystal Growth **42** 11 (1977)
17. J.S. Langer, H. Müller-Krumbhaar, Acta Met. **26** 1681 (1978)
18. J. Lipton, M.E. Glicksman, W. Kurz, Mat. Sci. Eng. **65** 57 (1984)
19. W. Kurz, B. Giovanola, R. Trivedi, Acta. Met. **34** 823 (1986)
20. J. Lipton, W. Kurz, R. Trivedi, Acta. Met. **35** 957 (1987)
21. A.T. Atwater, J.A. West, P.M. Smith, M.J. Aziz, J.Y. Tsao, P.S. Peercy, M.O. Thomson, Mater. Res. Soc. Symp. Proc. **157** 369 (1990)
22. B. Vinet, L. Cortella, J.J. Favier, P. Desre, Appl. Phys. Lett. **58** 97 (1991)
23. D. Orgassa, J. Laakmann, P.R. Sahm, Acta Met. Mat., submitted for publication
24. R. Willnecker, private communication, march 1995
25. M.A. Chopra, Ph. D. Thesis, Rensselaer Polytechnic Institute, Troy, New York (1983)
26. A. Ludwig, W. Kurz, Acta Met. Mat., submitted for publication
27. C.A. Wulff, E.F. Westrum, J. Phys. Chem. **67** 2376 (1963)
28. M.E. Glicksman, J.D. Ayers, R.J. Schäfer, unpublished research, NRL (1975), cited in: S.H. Davis in *Handbook of Crystal Growth*, Vol. 1B, 861, ed D.T.J. Hurle (Elsevier Science Publishers, Holland, 1993)
29. S.Y. Shiraishi, R.G. Ward, Can. Metall. Quart. **3** 117 (1964)